

# PSMA PET/CT with Glu-urea-Lys-(Ahx)-[<sup>68</sup>Ga(HBED-CC)] versus 3D CT volumetric lymph node assessment in recurrent prostate cancer

Frederik L. Giesel<sup>1,6</sup> · H. Fiedler<sup>1</sup> · M. Stefanova<sup>1</sup> · F. Sterzing<sup>2</sup> · M. Rius<sup>3,6</sup> · K. Kopka<sup>4</sup> · J. H. Moltz<sup>4</sup> · A. Afshar-Oromieh<sup>1</sup> · P. L. Choyke<sup>5</sup> · U. Haberkorn<sup>1,6</sup> · C. Kratochwil<sup>1</sup>

Received: 14 February 2015 / Accepted: 2 June 2015 / Published online: 11 July 2015  
© Springer-Verlag Berlin Heidelberg 2015

## Abstract

**Purpose** PET/CT with the PSMA ligand is a powerful new method for the early detection of nodal metastases in patients with biochemical relapse. The purpose of this retrospective investigation was to evaluate the volume and dimensions of nodes identified by Glu-urea-Lys-(Ahx)-[<sup>68</sup>Ga(HBED-CC)] (<sup>68</sup>Ga-PSMA-11) in the setting of recurrent prostate cancer.

**Methods** All PET/CT images were acquired 60±10 min after intravenous injection of <sup>68</sup>Ga-PSMA-11 (mean dose 176 MBq). In 21 patients with recurrent prostate cancer and rising PSA, 49 PSMA-positive lymph nodes were identified. Using semiautomated lymph node segmentation software, node volume and short-axis and long-axis dimensions were measured and compared with the maximum standardized uptake values (SUVmax). Round nodes greater than or equal to 8 mm were considered positive by morphological criteria alone. The percentage of nodes identified by elevated

SUVmax but not by conventional morphological criteria was determined.

**Results** The mean volume of <sup>68</sup>Ga-PSMA-11-positive nodes was 0.5 ml (range 0.2 – 2.3 ml), and the mean short-axis diameter was 5.8 mm (range 2.4 – 13.3 mm). In 7 patients (33.3 %) with 31 PSMA-positive nodes only 11 (36 %) were morphologically positive based on diameters >8 mm on CT. In the remaining 14 patients (66.7 %), 18 (37 %) of PSMA positive lymph nodes had short-axis diameters <8 mm with a mean short-axis diameter of 5.0 mm (range 2.4 – 7.9 mm). Thus, in this population, <sup>68</sup>Ga-PSMA-11 PET/CT detected nodal recurrence in two-thirds of patients who would have been missed using conventional morphological criteria.

**Conclusion** <sup>68</sup>Ga-PSMA-11 PET/CT is more sensitive than CT based 3D volumetric lymph node evaluation in determining the node status of patients with recurrent prostate cancer, and is a promising method of restaging prostate cancers in this setting.

**Keywords** <sup>68</sup>Ga-PSMA-11 PET/CT · Recurrent prostate cancer · Lymph node evaluation · Lymph node metastasis

✉ Frederik L. Giesel  
frederik@egiesel.com

<sup>1</sup> Department of Nuclear Medicine, INF 400, University Hospital Heidelberg, University of Heidelberg, 69120 Heidelberg, Germany

<sup>2</sup> Department of RadioOncology, University of Heidelberg, Heidelberg, Germany

<sup>3</sup> Institute for Transuranium Elements (ITU), European Commission, Karlsruhe, Germany

<sup>4</sup> Radiopharmaceutical Chemistry, German Cancer Research Center (dkfz), Heidelberg, Germany

<sup>5</sup> Molecular Imaging Program, National Cancer Institute, Bethesda, USA

<sup>6</sup> Cooperation Unit Nuclear Medicine, DKFZ, Heidelberg, Germany

## Introduction

The pelvic lymph nodes are a common site of recurrent prostate cancer after surgery or radiation. Evidence based largely on the levels of prostate-specific antigen (PSA) in biochemical recurrence indicate that the sooner treatment, typically consisting of radiation and androgen deprivation therapy (ADT), is instituted after detection, the better is survival [1]. This increases the importance of early detection and localization of recurrent disease, whether in the lymph nodes or in the prostatic bed (Figs. 1, 2, 3 and 4).

**Fig. 1** A 67-year-old patient with recurrent prostate cancer after prostatectomy. **a** The  $^{68}\text{Ga}$ -PSMA PET maximum intensity projection demonstrates multiple positive nodes in the pelvis abdomen, thorax and neck. **b–d** The CT image (**b**), PET/CT image (**c**) and PET image (**d**) show a single axial slice in the pelvis demonstrating three PSMA-positive nodes (*arrows*)

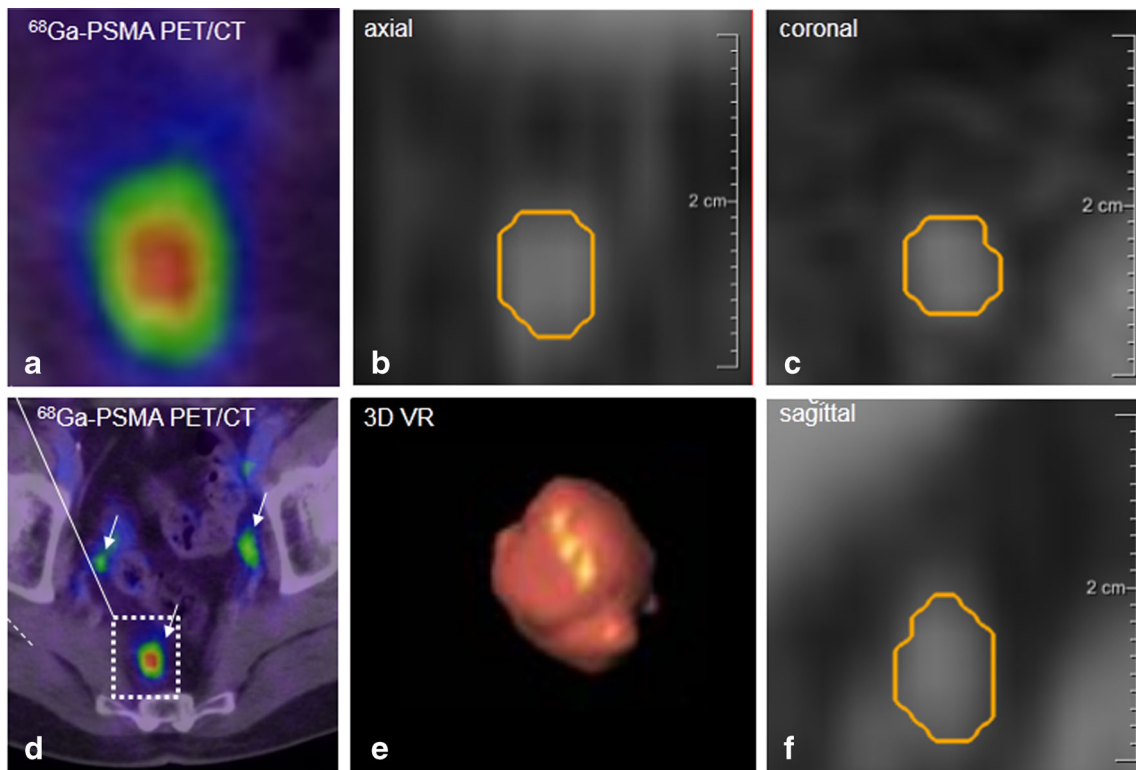
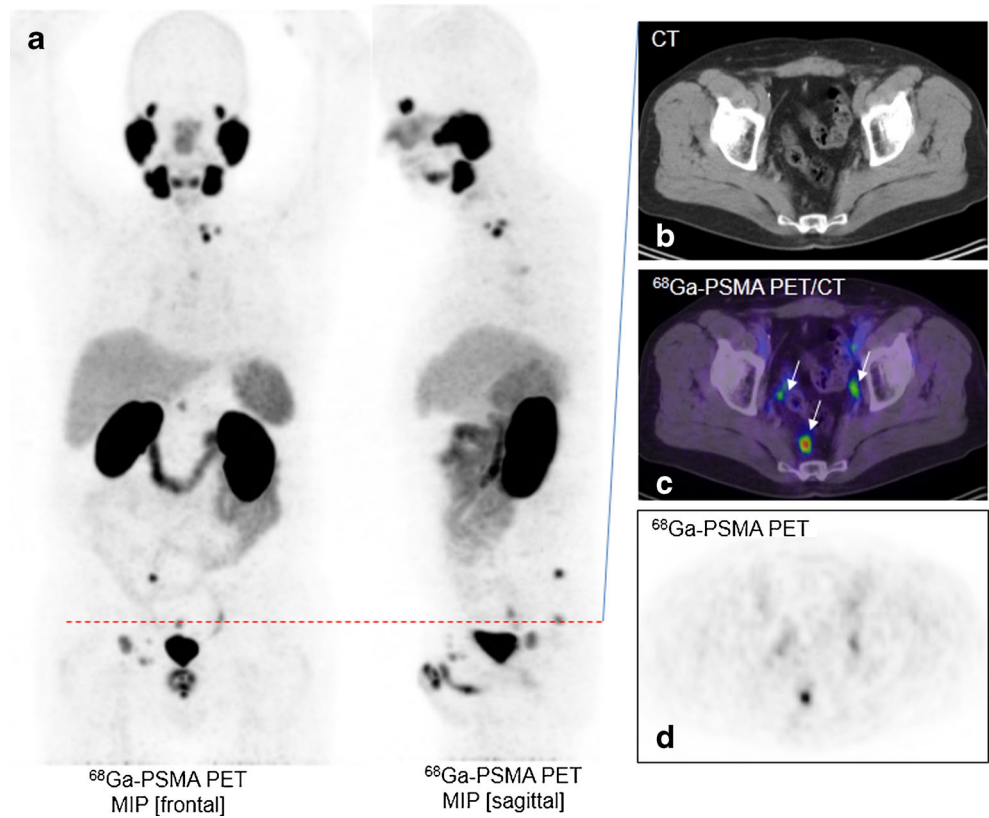


**Fig. 2** Image processing of a PSMA-positive node. The node corresponding to the positive  $^{68}\text{Ga}$ -PSMA PET images (**a**, **d** SUVmax 5.82) is represented on the CT images (**b** axial, **c** coronal, and **f** sagittal planes). It was segmented using Fraunhofer MEVIS software enabling

automated quantification of the dimensions (short-axis diameter 4.19 mm, long-axis diameter 6.76 mm). **e** Volume rendering of the segmented node also provided by the software

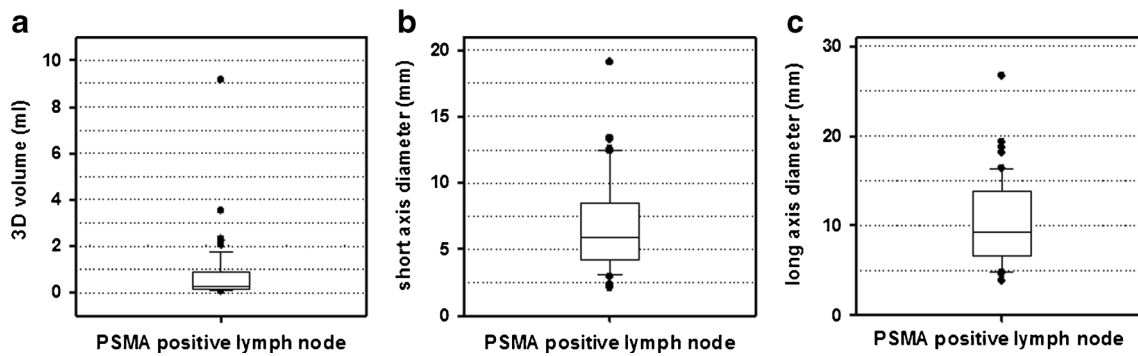


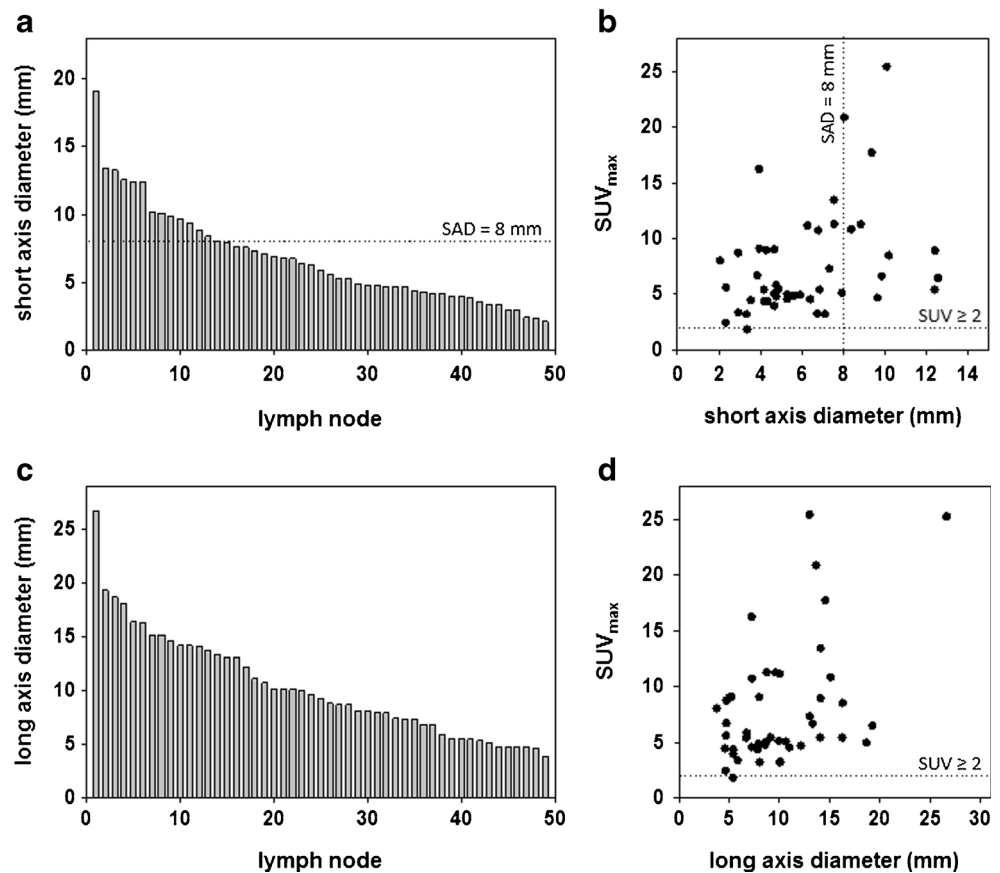
**Fig. 3** Volume (a), short-axis diameter (b) and long-axis diameter (c) of PSMA positive lymph nodes indicating that  $^{68}\text{Ga}$ -PSMA PET/CT is able to detect many metastatic nodes smaller than the standard size for positive lymph nodes on CT or MRI (diameter >1 cm, volume >0.5 cm<sup>3</sup>)

Current methods for assessing lymph nodes in the recurrence setting are limited. Although pelvic lymph node dissection is considered the most reliable procedure for assessing the presence of nodal invasion in the primary setting, this is often impractical in the recurrence setting [2]. CT is commonly used for nodal staging. However, CT has a limited ability to predict lymph node invasion because of its low sensitivity for small-volume or micrometastatic disease [3–5]. In order to avoid excessive false-positive findings, the normal upper limit of the short-axis diameter of pelvic lymph nodes is usually set at 7–10 mm depending on the location. However, up to 80 % of metastatic lymph nodes in prostate cancer have a short-axis

diameter less than 7 mm [3–6]. Similar comments apply to MRI which has classically relied on size criteria alone, although there has been recent interest in the use of diffusion-weighted MRI in this setting [7]. Thus, morphological criteria alone are highly limited in their ability to predict lymph node recurrence.

A new imaging method, PSMA PET/CT, has recently been introduced to evaluate prostate cancer. Prostate-specific membrane antigen (PSMA) is highly expressed in many prostate cancers and correlates with traditional negative prognostic factors such as a high Gleason score, metastasis or recurrent disease, but is not found in most other tissues [8]. Thus

**Fig. 4** Morphological distribution of all 49 PSMA-positive lymph nodes in terms of their short-axis diameter (a) and long-axis diameter (c). The relationships between SUV<sub>max</sub> and the short axis diameter (b) and long axis diameter (d) of the PSMA-positive lymph nodes are also shown



PSMA-targeted PET agents have considerably more specificity than conventional anatomic imaging. However, it is not clear that PET/CT with the  $^{68}\text{Ga}$ -PSMA ligand has superior sensitivity to CT alone, given the lower spatial resolution of PET in comparison with CT. For instance, typical PET scanners have a spatial resolution of 3–5 mm, whereas CT has submillimetre resolution, and it might be that only larger nodes are detectable by PET.

Therefore, we aimed to determine if PET/CT with  $^{68}\text{Ga}$ -PSMA-11 is capable of detecting nodal metastases below the conventional CT size thresholds for nodal metastasis.

## Materials and methods

### Patients

In this retrospective investigation we evaluated a total of 49 PET-positive lymph nodes in 21 consecutive patients (median age 70 years, range 54–79 years) referred to radiooncology with biochemical recurrence (i.e. rising PSA) of prostate cancer following radical prostatectomy (initial mean PSA level 6.84 ng/ml, range 0.6–45 ng/ml). The patients included in this investigation had a mean Gleason score of 8 (range 6–9). All patients the D'Amico risk category was intermediate or high at diagnosis (Table 1). All patients signed a written informed consent form for the purposes of anonymized evaluation and publication of their data. All reported investigations were conducted in accordance with the principles of the Declaration of Helsinki and with our national regulations. This evaluation was approved by the Ethics Committee of the University of Heidelberg.

### Image acquisition, PSMA PET analysis and volumetric CT histogram analysis

All PET/CT examinations were done on a Biograph 6 PET/CT scanner (Siemens/CTI). Imaging was started  $60 \pm 10$  min after intravenous injection of  $^{68}\text{Ga}$ -PSMA-11 at a median dose of 176 MBq (range 79–317 MBq). For attenuation correction of the PET scan, a CT scan (130 keV, 80 mAs; CareDose) without contrast medium was performed. Static emission scans, corrected for dead time, scatter and decay, were acquired from the vertex to the proximal legs, requiring eight bed positions with 3 min per bed position. The images were iteratively reconstructed with the OSEM algorithm using four iterations with eight subsets and Gaussian filtering to an in-plane spatial resolution of 5 mm at full-width at half-maximum. For calculation of the standardized uptake value (SUV), circular regions of interest were drawn around the area with focally increased uptake in transaxial slices and automatically adapted to a three-dimensional volume of interest with e.soft software (Siemens) at a 70 % isocontour. The CT scan was

reconstructed with a B30 kernel to a slice thickness of 5 mm with an increment of 2.5 mm. Lymph nodes were considered PSMA-positive when the maximum SUV (SUV<sub>max</sub>) was  $>2$ . This cut-off value was chosen after evaluating the blood pool at 60 min after injection in the aorta, which was found to have a mean  $\pm$  standard deviation SUV<sub>max</sub> of  $1.49 \pm 0.49$ .

Volumetric CT analysis was performed on PET-positive nodes using semiautomated software (Fraunhofer MEVIS, Bremen, Germany) that segments the nodes and automatically determines mean density, short-axis diameter, long-axis diameter and volume. Semiautomatic three-dimensional histogram analysis is initiated after the user provided a seed point in the lymph node and the software found the margins of the node. The segmentation starts with a fixed-width thresholding around the seed point. To remove attached vessels, muscles or other lymph nodes, a watershed transform is performed on the distance map of the thresholding result. The watershed transform is controlled by include and exclude markers which are set according to an ellipsoid approximation of the lymph node. The volumes were evaluated by a radiologist to ensure that no extraneous tissue was segmented and manually corrected in all three dimensions, if necessary.

### Statistical evaluation

Nodes with a diameter more than 8 mm were accepted as positive for metastasis on CT [9, 10]. Descriptive statistics defining the percent positive PET/CT scans with nodes smaller than the above size criteria were calculated. Pearson coefficients were calculated using Excel (Microsoft, Seattle, WA).

## Results

A total of 49 lymph nodes in 21 patients could clearly be correlated with nodal uptake on  $^{68}\text{Ga}$ -PSMA ligand PET/CT. By study definition all 49 lymph nodes demonstrated  $^{68}\text{Ga}$ -PSMA ligand uptake on PET/CT with a mean SUV<sub>max</sub> of 7.43 (range 1.8–25.2). Among the 49 PSMA-positive lymph nodes, 38 (78 %) were morphologically negative ( $<8$  mm) and 11 (22 %) were morphologically positive on conventional imaging ( $\geq 8$  mm) (Fig. 4). All 49 lymph nodes were analysed with the semiautomated segmentation software. Semiautomatic segmentation required less than 5 min per patient but enabled derivation of several important parameters: lymph-node size (short and long axis) and lymph-node volume. The interobserver and intraobserver reproducibility was good with a coefficient of variation  $<5$  % when the software was evaluated for reliability in a recent study [11].

The mean volume of all 49 lymph nodes was 0.5 ml (range 0.2–2.3 ml), the mean short-axis diameter was 5.8 mm (range 2.4–13.3 mm) and the mean long axis diameter was 9.5 mm (range 4.7–19.3 mm). In seven patients (33 %) at least one

**Table 1** Patient demographics

| Patient no. | Age at PSMA PET/CT (years) | Initial PSA level (ng/ml) | Initial Gleason score | Risk (d'Amico category) | SUVmax |
|-------------|----------------------------|---------------------------|-----------------------|-------------------------|--------|
| 1           | 54                         | 5.6                       | 6                     | High                    | 8.7    |
| 2           | 75                         | 2.7                       | 7                     | Intermediate            | 6.2    |
| 3           | 75                         | 10.6                      | 8                     | High                    | 4.9    |
| 4           | 65                         | 1.6                       | 7                     | Intermediate            | 4.5    |
| 5           | 79                         | 3.1                       | 9                     | High                    | 3.1    |
| 6           | 78                         | 2.7                       | 9                     | High                    | 4.9    |
| 7           | 75                         | 3.8                       | 7                     | Intermediate            | 6.9    |
| 8           | 70                         | 2.33                      | 8                     | High                    | 12.1   |
| 9           | 71                         | 2.77                      | 7                     | Intermediate            | 13.1   |
| 10          | 70                         | 7.2                       | 9                     | High                    | 6.7    |
| 11          | 71                         | 1.4                       | 8                     | High                    | 2.4    |
| 12          | 69                         | 5.88                      | 7                     | Intermediate            | 3.14   |
| 13          | 62                         | 1.35                      | 9                     | High                    | 3.8    |
| 14          | 59                         | 45                        | 7                     | Intermediate            | 25.2   |
| 15          | 63                         | 0.62                      | 6                     | Intermediate            | 4.3    |
| 16          | 72                         | 12                        | 9                     | High                    | 15.5   |
| 17          | 69                         | 0.8                       | 7                     | Intermediate            | 4.3    |
| 18          | 78                         | 1.8                       | 7                     | Intermediate            | 9.8    |
| 19          | 55                         | 6.4                       | 8                     | High                    | 8.9    |
| 20          | 63                         | 25.4                      | 8                     | High                    | 5.6    |
| 21          | 68                         | 0.64                      | 7                     | High                    | 1.8    |

node was larger than the conventional criteria for morphological positivity. However, among the 31 PSMA-positive nodes in these patients only 11 (36 %) were  $\geq 8$  mm on the CT scan with a mean short-axis diameter of 11.8 mm (range 8.4–19.1 mm). None of 14 patients (67 %) with 18 PSMA-positive lymph nodes met the morphological criteria for positivity. In this group, the mean short-axis diameter was 5.0 mm (range 2.4–7.9 mm) and the mean PSMA SUVmax was 5.5 (range 1.8–13.1). Thus, the N stage was changed from N0 to N1 in 14 of 21 patients (67 %) in this cohort on  $^{68}\text{Ga}$ -PSMA ligand PET/CT.

## Discussion

PSA testing after surgery or radiation therapy for prostate cancer permits the early identification of patients with biochemical recurrence. There is evidence that early treatment may result in better outcomes [1]. However, localization of the site of recurrence has proven to be difficult and thus empirical therapies such as pelvic irradiation and ADT have been employed. However, such treatments are given without specific regard to the location of the recurrence. Localizing the exact sites of recurrence could permit a more targeted approach with fewer side effects. In patients with single lesions surgery with curative intent may be performed although this is

controversial. Other options include targeted ablation, focal radiation and even molecular and immunomodulatory therapies. Missing from the current clinical decision tree, however, is an effective means of detecting and monitoring recurrence sites while this “therapeutic window” is still open.

A common site of recurrent disease in prostate cancer is the pelvic lymph nodes. However, the existing methods for detection of nodes such as CT or MRI are nonspecific. Enlargement of round nodes beyond 8 mm is considered a positive finding with a low sensitivity of approximately 34–40 % and a moderate/high specificity (80–97 %) [9, 10, 12]. Just as small nodes below the size threshold are commonly missed, large lymph nodes above the size threshold may simply represent nodal hyperplasia. For this reason, CT and MRI are not considered reliable enough for routine nodal staging [2]. A source of considerable error in studies of lymph nodes is the variability in the manual measurement of lymph node size. Volumetric analysis allows a more precise and objective assessment of tumour burden. It was first introduced for pulmonary nodules and recently was made clinically available with special software packages [13]. CT volumetric analysis software (Fraunhofer MEVIS) was used to precisely determine nodal volume. This enabled reliable and rapid nodal measurements in this study.

As reported recently, enhanced uptake of  $^{68}\text{Ga}$ -PSMA-11 correlated well with the surgical pathology in 42 patients [14].

In 319 patients evaluated with follow-up as the standard of reference, sensitivity and specificity were found to be 76.6 % and 100 %, and the negative and positive predictive values were 91.4 % and 100 %, respectively [14]. Due to the positive predictive value of 100 % in this large study with a thoroughly defined gold standard, a positive PSMA PET was considered as the standard of reference for lymph node involvement in our investigation. Nevertheless, PSMA is not specific for prostate cancer but can also be found in the neovasculature of other solid tumours (thyroid, colon, kidney, glioblastoma). Thus, false-positive lymph node metastases can occur in patients with secondary malignancies. Nevertheless, the likelihood that PSMA-positive lymph nodes found in the typical lymph drainage region of the prostate are true-positive can be considered to be close to 100 %. In our small patient population we did not observe PET-positive lymph nodes in uncommon locations, which would have to be interpreted more cautiously with regard to the possibility of a second malignancy.

In this analysis, 21 patients with recurrent prostate cancer who underwent  $^{68}\text{Ga}$ -PSMA-11 PET/CT were evaluated. Among the 21 patients, only 7 (33 %) harboured nodes that exceeded the size criterion for metastases on CT. This is consistent with existing data on the sensitivity of CT. However, the remaining 14 patients who were considered normal by CT criteria were actually shown to harbour metastases in small nodes not meeting the size criterion for positivity on CT. Further, only 11 (22.45 %) of the 49 PSMA-positive nodes met the size criterion for metastasis on CT. Thus, using standard TNM staging only one-third of the patients in this study would have been considered cN1 by CT criteria. The use of PSMA PET/CT imaging led to the reclassification of another 14 patients from cN0 to cN1. In a previous study evaluating patients with prostate cancer prior to first-line radiotherapy,  $^{68}\text{Ga}$ -PSMA-11 PET/CT led to a change in TNM staging due to a change from cN0 to cN1 in nearly 40 % of patients. This result is in line with the results of our current investigation [15].

In the past, other PET imaging tracers have also been used in the setting of biochemical recurrence.  $^{11}\text{C}$ -Choline is one such agent that has shown variable success in this setting [13, 16, 17]. Other PET tracers include  $^{18}\text{F}$ -fluoromethyl choline ( $^{18}\text{F}$ -FMCh),  $^{18}\text{F}$ -fluoroethyl choline ( $^{18}\text{F}$ -FECh),  $^{11}\text{C}$ -acetate,  $^{18}\text{F}$ -FACBC (radiofluorinated aminocyclobutane carboxylic acid) and  $^{18}\text{F}$ -FDHT (radiofluorinated dihydrotestosterone), but none has emerged as clearly superior to any other. Our initial experience with  $^{68}\text{Ga}$ -PSMA-11 PET/CT suggests that this novel tracer can detect relapses and metastases with high contrast by binding to the extracellular catalytic domain of PSMA, followed by internalization [18, 19].

A significant advantage of PSMA PET/CT is that PSMA-11 uptake in lymph node and other soft tissue metastases is higher than that of other agents [19–21]. Another promising recently introduced PSMA ligand labelled with  $^{18}\text{F}$  showed

similar contrast ratios in a small cohort of seven patients [22]. A potential disadvantage is that tumoral PSMA expression may be modulated by the androgen receptor. In preclinical studies based on cell lines, antiandrogens initially upregulated PSMA expression [22] while prolonged ADT seemed to downregulate PSMA over time [23, 24] but might also induce upregulation after ADT is withdrawn [14]. In contrast,  $^{68}\text{Ga}$ -PSMA-11 PET/CT was more frequently positive in patients receiving ADT at the time of the scan than in patients without such treatment [25]. Thus further clinical studies are necessary to draw a final conclusion on the impact of ADT on the expression of tumour PSMA in humans.

## Conclusion

In this study, two-thirds of patients with recurrent prostate cancer were upstaged from cN0 to cN1 based on their  $^{68}\text{Ga}$ -PSMA-11 PET/CT scan. The majority (78 %) of nodes detected by  $^{68}\text{Ga}$ -PSMA-11 PET/CT were smaller than 8 mm in diameter and therefore did not meet standardized morphological criteria for metastatic nodes. Thus,  $^{68}\text{Ga}$ -PSMA-11 PET/CT appears to be a promising method of restaging patients with suspected recurrent prostate cancer based on elevated PSA levels. The ability of  $^{68}\text{Ga}$ -PSMA-11 PET/CT to detect focal sites of disease in recurrent prostate cancer with high sensitivity opens the possibility for early targeted therapies. In the case of single lesions, a surgical approach may be considered, although data are currently sparse. Other options include targeted ablative technologies or focal radiation. Further investigations are necessary to demonstrate which of these treatment modalities can really benefit from improved diagnostic sensitivity.

## Compliance with ethical standards

**Funding** This research was supported by the Klaus-Tschira-Stiftung (project no. 00.198.2012).

**Conflicts of interest** None.

**Ethical approval** All procedures performed in this study were in accordance with the ethical standards of the institutional research committee and the national regulations and also with the principles of the 1964 Declaration of Helsinki and its later amendments as far as they are required for this type of retrospective study.

**Informed consent** Informed consent was obtained from all patients.

## References

1. Kwon O, Kim KB, Lee YI, Byun SS, Kim JS, Lee SE, et al. Salvage radiotherapy after radical prostatectomy: prediction of biochemical

- outcomes. *PLoS One*. 2014;9(7), e103574. doi:10.1371/journal.pone.0103574.2.
2. Heidenreich A, Bellmunt J, Bolla M, Joniau S, Mason M, Matveev V, et al. EAU guidelines on prostate cancer. Part 1: screening, diagnosis, and treatment of clinically localised disease. *Eur Urol*. 2011;59:61–71.
  3. Hövels AM, Heesakkersb RA, Adang EM, Jager GJ, Strum S, Hoogeveen YL, et al. The diagnostic accuracy of CT and MRI in the staging of pelvic lymph nodes in patients with prostate cancer: a meta-analysis. *Clin Radiol*. 2008;63:387–95. doi:10.1016/j.crad.2007.05.0224.
  4. Engeler CE, Wasserman NF, Zhang G. Preoperative assessment of prostatic carcinoma by computerized tomography. Weaknesses and new perspectives. *Urology*. 1992;40:346–50.
  5. Flanigan RC, McKay TC, Olson M, Shankey TV, Pyle J, Waters WB. Limited efficacy of preoperative computed tomographic scanning for the evaluation of lymph node metastasis in patients before radical prostatectomy. *Urology*. 1996;48:428–32.
  6. Hilton S, Herr HW, Teitcher JB, Begg CB, Castellino RA. CT detection of retroperitoneal lymph node metastases in patients with clinical stage I testicular nonseminomatous germ cell cancer: assessment of size and distribution criteria. *AJR Am J Roentgenol*. 1997;169:521–5.
  7. Thoeny HC, Froehlich JM, Triantafulloy M, Huesler J, Bains LJ, Vermathen P, et al. Metastases in normal-sized pelvic lymph nodes: detection with diffusion-weighted MR imaging. *Radiology*. 2014;273(1):125–35. doi:10.1148/radiol.14132921.
  8. Eder M, Eisenhut M, Babich J, Haberkorn U. PSMA as a target for radiolabelled small molecules. *Eur J Nucl Med Mol Imaging*. 2013;40:819–23. doi:10.1007/s00259-013-2374-2.
  9. Torabi M, Aquino SL, Harisinghani MG. Current concepts in lymph node imaging. *J Nucl Med*. 2004;45:1509–18.
  10. Tempany CM, Zou KH, Silverman SG, Brown DL, Ab K, McNeil BJ. Staging of advanced ovarian cancer: comparison of imaging modalities – report from the Radiological Diagnostic Oncology Group. *Radiology*. 2000;215:761–7.
  11. Moltz JM, Bornemann L, Kuhnigk JM, Dicken V, Peitgen E, Meier S, et al. Advanced segmentation techniques for lung nodules, liver metastases, and enlarged lymph nodes in CT scans. *IEEE J Sel Topics Signal Process*. 2009;3:122–34.
  12. McMahon CJ, Rofsky NM, Pedrosa I. Lymphatic metastases from pelvic tumors: anatomic classification, characterization and staging. *Radiology*. 2010;254:31–46. doi:10.1148/radiol.2541090361.
  13. Maleike D, Fabel M, Tetzlaff R, von Tengg-Kobligk H, Heimann T, Meinzer HP, et al. Lymph node segmentation on CT images by a shape model guided deformable surface method. *Proc SPIE*. 2008;6914:69141S. doi:10.1117/12.770352
  14. Wright GL, Mayer Grob B, Haley C, Grossman K, Newhall K, Petrylak D, et al. Upregulation of prostate-specific membrane antigen after androgen-deprivation therapy. *Urology*. 1996;48(2):326–34.
  15. Sterzing F, Fiedler H, Stefanova M, Afshar-Oromieh A, Kratochwil C, et al. Impact of 68Ga-PSMA PET/CT in staging of prostate cancer patient prior to radiation therapy. *Int J Radiat Oncol Biol Phys*. 2014;90(1):S449. doi:10.1016/j.ijrobp.2014.05.1407.
  16. Heesakkers RA, Hovels AM, Jager GJ, van den Bosch HC, Witjes JA, Raat HP, et al. MRI with a lymph-node-specific contrast agent as an alternative to CT scan and lymph-node dissection in patients with prostate cancer: a prospective multicohort study. *Lancet Oncol*. 2008;9:850–6. doi:10.1016/S1470-2045(08)70203-1.
  17. Schiavina R, Scattoni V, Castellucci P, Picchio M, Corti B, Briganti A, et al. 11C-choline positron emission tomography/computerized tomography for preoperative lymph-node staging in intermediate-risk and high-risk prostate cancer: comparison with clinical staging nomograms. *Eur Urol*. 2008;54:392–401. doi:10.1016/j.eururo.2008.04.030.
  18. Afshar-Oromieh A, Malcher A, Eder M, Eisenhut M, Linhart HG, Hadaschik BA, et al. PET imaging with a [(68)Ga]gallium-labelled PSMA ligand for the diagnosis of prostate cancer: biodistribution in humans and first evaluation of tumour lesions. *Eur J Nucl Med Mol Imaging*. 2013;40:486–95. doi:10.1007/s00259-013-2386-y.
  19. Afshar-Oromieh A, Zechmann CM, Malcher A, Eder M, Eisenhut M, Linhart HG, et al. Comparison of PET imaging with a (68)Ga-labelled PSMA ligand and (18)F-choline-based PET/CT for the diagnosis of recurrent prostate cancer. *Eur J Nucl Med Mol Imaging*. 2014;41(1):11–20. doi:10.1007/s00259-013-2525-5.
  20. Hacker A, Jeschke S, Leeb K, Prammer K, Ziegerhofer J, Segal W, et al. Detection of pelvic lymph node metastases in patients with clinically localized prostate cancer: comparison of 18F-fluorocholine positron emission tomography-computerized tomography and laparoscopic radioisotope guided sentinel lymph node dissection. *J Urol*. 2006;176(5):2014–8.
  21. Husarik DB, Miralbell R, Dubs M, John H, Giger OT, Gelet A, et al. Evaluation of [(18)F]-choline PET/CT for staging and restaging of prostate cancer. *Eur J Nucl Med Mol Imaging*. 2008;35(2):253–63.
  22. Szabo Z, Mena E, Rowe SP, Plyku D, Nidal R, Eisenberger MA, et al. Initial evaluation of [18F]DCFPyL for prostate-specific membrane antigen (PSMA)-targeted PET imaging of prostate cancer. *Mol Imaging Biol*. 2015. doi:10.1007/s11307-015-0850-8
  23. Evans MJ, Smith-Jones PM, Wongvipat J, Navarro V, Kim S, Bander NH, et al. Noninvasive measurement of androgen receptor signaling with a positron-emitting radiopharmaceutical that targets prostate-specific membrane antigen. *Proc Natl Acad Sci U S A*. 2011;108(23):9578–82. doi:10.1073/pnas.1106383108.
  24. Liu T, Wu LY, Fulton MD, Johnson JM, Berkman C. Prolonged androgen deprivation leads to down regulation of androgen receptor and prostate specific membrane antigen in prostate cancer cells. *Int J Oncol*. 2012;41(6):2087–92. doi:10.3892/ijo.2012.1649.
  25. Afshar-Oromieh A, Avtzi E, Giesel FL, Holland Letz T, Linhart HG, Eder M, et al. The diagnostic value of PET/CT imaging with the 68Ga-labelled PSMA ligand HBED-CC in the diagnosis of recurrent prostate cancer. *Eur J Nucl Med Mol Imaging*. 2015;42(2):197–209. doi:10.1007/s00259-014-2949-6.
  26. Budiharto T, Joniau S, Lerut E, Van den Bergh L, Mottaghy R, Deroose CM, et al. Prospective evaluation of 11C-choline positron emission tomography/computed tomography and diffusion-weighted magnetic resonance imaging for the nodal staging of prostate cancer with a high risk of lymph node metastases. *Eur Urol*. 2011;60:125–30. doi:10.1016/j.eururo.2011.01.015.